SAND2024-01300J

Quantum tracking control of the orientation of symmetric top molecules

Alicia B. Magann,[1,2,*] Tak-San Ho,[3] Christian Arenz,[3,4] and Herschel A. Rabitz[3,†]

[1]*Department of Chemical & Biological Engineering, Princeton University, Princeton, New Jersey 08544, USA*

[2]*Center for Computing Research, Sandia National Laboratories, Albuquerque, New Mexico 87185, USA*

[3]*Department of Chemistry, Princeton University, Princeton, New Jersey 08544, USA*

[4]*School of Electrical, Computer and Energy Engineering, Arizona State University, Tempe, Arizona 85281, USA*

(Dated: February 6, 2024)

The goal of quantum tracking control is to identify shaped fields to steer observable expectation values along designated time-dependent tracks. The fields are determined via an iteration-free procedure, which is based on inverting the underlying dynamical equations governing the controlled observables. In this article, we generalize the ideas in Phys. Rev. A 98, 043429 (2018) to the task of orienting symmetric top molecules in 3D. To this end, we derive equations for the control fields capable of directly tracking the expected value of the 3D dipole orientation vector along a desired path in time. We show this framework can be utilized for tracking the orientation of linear molecules as well, and present numerical illustrations of these principles for symmetric top tracking control problems.

I. INTRODUCTION

The desire to selectively manipulate molecular dynamics using external fields is a decades-old dream that has motivated a broad range of research pursuits [1–3], including the development of quantum optimal control (QOC) theory [4]. The goal of QOC is to identify fields to control the dynamics of a quantum system, such that the system achieves a desired control objective at a designated target time $t = T$. The task of identifying an optimal field is typically accomplished by iterative optimization methods [5–7]. Although these methods can be computationally demanding, QOC has nonetheless found broad applications, ranging from quantum computing [8–14] to chemical reactions [15–19].

In this article, we focus on another formulation, quantum tracking control (QTC) [20–22], for designing control fields to accurately track the temporal path of an observable of interest. The origins of QTC are in engineering control theory, which has explored tracking control in a range of settings including linear [23], nonlinear [24], and bilinear [25] systems. For quantum-mechanical applications, tracking control principles have been applied towards the numerical study of systems including a qubit [26], a single atom [27], and various molecular [20–22, 28, 29] and solid-state systems [30–32].

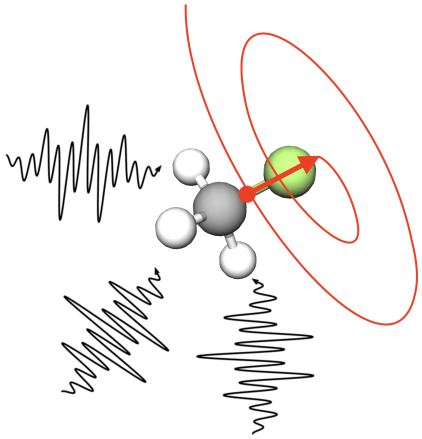

Figure 1. In this article, we formulate QTC for controlling the 3D orientation of symmetric top molecules, such as fluoromethane, shown here. The control procedure involves designing three orthogonal fields (black) in order to drive the molecule's 3D dipole vector along a desired time-dependent track (red). The three fields can be determined by solving an inverse equation, without the need for optimization.

The aim of QTC is to find tracking control field(s) $\boldsymbol{\varepsilon}(t)$ that drive one or multiple observable expectation values $\langle \boldsymbol{O} \rangle(t) \equiv \langle \psi(t) | \boldsymbol{O} | \psi(t) \rangle$ along desired time-dependent "tracks" $\langle \boldsymbol{O} \rangle_d(t)$ for a chosen time interval $t \in [0, T]$. This is carried out by directly inverting the underlying dynamical equation governing $\langle \boldsymbol{O} \rangle(t)$ in order to solve for $\boldsymbol{\varepsilon}(t)$ [20–22]. We remark that QTC possesses similarities to reverse engineering [33–35], which aims to obtain

* abmagan@sandia.gov
† hrabitz@princeton.edu

an analytical form for $\boldsymbol{\varepsilon}(t)$ that achieves desired trajectories of the state. However, reverse engineering is typically restricted to very small or simple systems. Because it does not require any iterative optimization, QTC can be computationally advantageous compared with usual QOC schemes.

A challenge facing QTC is the potential presence of singularities in the corresponding direct inversion procedure [36]. That is, attempts to exactly track arbitrary time-dependent observable paths can produce unphysical, discontinuous control fields [37] and deviations from the desired tracks. However, if singularities can be avoided, QTC offers an appealing, iteration-free approach for designing fields to control quantum systems.

Here, we consider applications of QTC to rotational control, for the purpose of orienting symmetric top molecules. Quantum control of rotational dynamics has been explored in the context of numerous applications [38]. In particular, quantum control of molecular orientation has been explored for applications spanning high harmonic generation [39] and chemical reaction enhancement [40–42], and has been the subject of numerous experimental [43–45] and theoretical [46–52] studies. In particular, QTC of molecular rotor orientation in 2D has been explored [28]. In this work, we extend this prior work to linear and symmetric top molecules in 3D. We note that although the controllability of linear and symmetric top molecules has been the subject of other studies [53, 54], to the best of our knowledge, the suitability of symmetric tops for QTC has thus far not been explored.

The remainder of the paper is organized as follows. We begin by outlining the symmetric top rotor model and derive QTC equations for the control fields to track its orientation. We go on to describe computational methods for solving the QTC equations by expanding the wave function in terms of angular momentum eigenfunctions of the symmetric top and address the QTC singularity issue. We then show how the formulation of QTC for symmetric top molecules can be reduced to the case of a linear rotor. We conclude with numerical illustrations and an outlook.

II. SYMMETRIC TOP MOLECULES IN 3D

We consider a symmetric top molecule with dynamics governed by the time-dependent Schrödinger equation,

$$i\frac{\partial}{\partial t}|\psi(t)\rangle = H(t)|\psi(t)\rangle\,, \tag{1}$$

where $\hbar = 1$ and the time-dependent Hamiltonian is

$$H(t) = H_0 - \boldsymbol{\mu}\cdot\boldsymbol{\varepsilon}(t) \tag{2}$$

in terms of (1) the field-free Hamiltonian H_0, (2) three orthogonal control fields $\varepsilon_X(t)$, $\varepsilon_Y(t)$, and $\varepsilon_Z(t)$, i.e., where $\boldsymbol{\varepsilon}(t) = \hat{X}\varepsilon_X(t) + \hat{Y}\varepsilon_Y(t) + \hat{Z}\varepsilon_Z(t)$, and (3) the components of the dipole moment $\boldsymbol{\mu} = \hat{X}\mu_X + \hat{Y}\mu_Y + \hat{Z}\mu_Z$, where $\hat{X}$, $\hat{Y}$, and $\hat{Z}$ denote the three Cartesian unit vectors in the laboratory, space-fixed frame of reference.

Given the symmetry of the molecule, the dipole moment is along the principal, molecular, body-fixed $\hat{z}$-axis, such that $\boldsymbol{\mu} = \hat{z}\mu_z$, where $\mu_z = \mu z$, μ is the magnitude of the dipole moment, and z is the body-fixed position operator. Noting that vectors represented in body-fixed coordinates $\hat{x}$, $\hat{y}$, and $\hat{z}$ and space-fixed coordinates $\hat{X}$, $\hat{Y}$, and $\hat{Z}$ can be related via Euler angles $\theta \in [0, \pi]$, $\phi \in [0, 2\pi]$, and $\chi \in [0, 2\pi]$, as per Fig. 2, the components of the dipole moment in the space-fixed frame are then given by

$$\begin{aligned}
\mu_X &= \mu X = \mu \sin\theta\cos\phi,\\
\mu_Y &= \mu Y = \mu \sin\theta\sin\phi,\\
\mu_Z &= \mu Z = \mu\cos\theta,
\end{aligned} \tag{3}$$

where X, Y, Z denote the space-fixed position operators, expressed using Euler angles θ, ϕ.

The molecule is assumed to be a rigid rotor, and the field-free symmetric top Hamiltonian is given by [55]

$$H_0 = B(J_x^2 + J_y^2) + CJ_z^2, \tag{4}$$

where B and C are rotational constants and J_x, J_y, and J_z, respectively, denote angular momentum projection

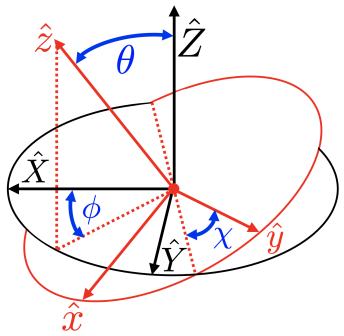

Figure 2. Diagram showing (θ, ϕ, χ) Euler angle relations between laboratory space-fixed $\hat{X}$, $\hat{Y}$, and $\hat{Z}$ coordinates (black) and molecular body-fixed $\hat{x}$, $\hat{y}$, and $\hat{z}$ coordinates (red).

operators in the molecular frame, given by the relations

$$J_x = -i\cos\chi\left(\cot\theta\frac{\partial}{\partial\chi} - \frac{1}{\sin\theta}\frac{\partial}{\partial\phi}\right) - i\sin\chi\frac{\partial}{\partial\theta},$$
$$J_y = i\sin\chi\left(\cot\theta\frac{\partial}{\partial\chi} - \frac{1}{\sin\theta}\frac{\partial}{\partial\phi}\right) - i\cos\chi\frac{\partial}{\partial\theta}, \tag{5}$$

and

$$J_z = -i\frac{\partial}{\partial\chi}. \tag{6}$$

As a result, the total angular momentum can be written as

$$\mathbf{J}^2 = -\left(\frac{\partial^2}{\partial\theta^2} + \cot\theta\frac{\partial}{\partial\theta} + \frac{1}{\sin^2\theta}\left(\frac{\partial^2}{\partial\phi^2} + \frac{\partial^2}{\partial\chi^2} - 2\cos\theta\frac{\partial^2}{\partial\phi\partial\chi}\right)\right) \tag{7}$$

and the field-free Hamiltonian becomes

$$H_0 = -B\left(\frac{\partial^2}{\partial\theta^2} + \cot\theta\frac{\partial}{\partial\theta} + \cot^2\theta\frac{\partial^2}{\partial\chi^2} - 2\frac{\cot\theta}{\sin\theta}\frac{\partial^2}{\partial\chi\partial\phi} + \frac{1}{\sin^2\theta}\frac{\partial^2}{\partial\phi^2}\right) - C\frac{\partial^2}{\partial\chi^2}. \tag{8}$$

III. QUANTUM TRACKING CONTROL EQUATIONS FOR SYMMETRIC TOP ORIENTATION

Here, we apply the QTC framework [20–22, 28] to tracking a symmetric top molecule's 3D orientation using three orthogonal QTC fields. The time-dependent symmetric top orientation is defined as

$$\langle\mathbf{R}\rangle(t) = \hat{X}\langle X\rangle(t) + \hat{Y}\langle Y\rangle(t) + \hat{Z}\langle Z\rangle(t), \tag{9}$$

which is the instantaneous expectation value, at time t, of the position vector operator $\mathbf{R} \equiv \hat{X}X + \hat{Y}Y + \hat{Z}Z$. By differentiating $\langle\mathbf{R}\rangle(t)$ with respect to t once we obtain

$$\frac{d\langle\mathbf{R}\rangle(t)}{dt} = i\langle[H_0, \mathbf{R}]\rangle(t), \tag{10}$$

which has no explicit dependence on $\boldsymbol{\varepsilon}(t)$. By further differentiating Eq. (10) with respect to t we obtain

$$\frac{d^2\langle\mathbf{R}\rangle(t)}{dt^2} = \langle[\boldsymbol{\mu}\cdot\boldsymbol{\varepsilon}(t), [H_0, \mathbf{R}]]\rangle(t) - \langle[H_0, [H_0, \mathbf{R}]]\rangle(t). \tag{11}$$

Eq. (11) can be expressed as a single matrix equation $\mathbf{b}(t) = \mathbf{A}(t)\boldsymbol{\varepsilon}(t)$, where $\boldsymbol{\varepsilon}(t) = (\varepsilon_X(t), \varepsilon_Y(t), \varepsilon_Z(t))^T$, the components of the matrix $\mathbf{A}(t)$ are given by

$$\begin{aligned}
\mathbf{A}_{X,X}(t) &= \langle[\mu_X, [H_0, X]]\rangle(t) = 2\mu B\langle Y^2 + Z^2\rangle(t)\\
\mathbf{A}_{Y,Y}(t) &= \langle[\mu_Y, [H_0, Y]]\rangle(t) = 2\mu B\langle Z^2 + X^2\rangle(t)\\
\mathbf{A}_{Z,Z}(t) &= \langle[\mu_Z, [H_0, Z]]\rangle(t) = 2\mu B\langle X^2 + Y^2\rangle(t)\\
\mathbf{A}_{X,Y}(t) &= \mathbf{A}_{Y,X}(t) = \langle[\mu_Y, [H_0, X]]\rangle(t)\\
&= -2\mu B\langle XY\rangle(t)\\
\mathbf{A}_{Y,Z}(t) &= \mathbf{A}_{Z,Y}(t) = \langle[\mu_Z, [H_0, Y]]\rangle(t)\\
&= -2\mu B\langle YZ\rangle(t)\\
\mathbf{A}_{Z,X}(t) &= \mathbf{A}_{X,Z}(t) = \langle[\mu_X, [H_0, Z]]\rangle(t)\\
&= -2\mu B\langle ZX\rangle(t),
\end{aligned} \tag{12}$$

and the components of the vector $\mathbf{b}(t)$ read

$$\mathbf{b}(t) = \frac{d^2\langle\mathbf{R}\rangle_d(t)}{dt^2}\langle + \langle[H_0, [H_0, \mathbf{R}]]\rangle(t). \tag{13}$$

Here the subscript "d" denotes the predefined or "designated" path in time to be tracked, $\langle\mathbf{R}\rangle_d(t)$.

The QTC fields can be found by inverting $\mathbf{A}(t)$, i.e., assuming the inverse of $\mathbf{A}(t)$ exists at all times t, and solving the resultant QTC equations,

$$\boldsymbol{\varepsilon}(t) = \mathbf{A}^{-1}(t)\mathbf{b}(t), \tag{14}$$

as follows. First, the initial field values $\boldsymbol{\varepsilon}(0)$ are computed at time $t = 0$, by evaluating (14) for an initial state $|\psi(0)\rangle$. The next step is to evolve the system forward in time by integrating the Schrödinger equation (1) over a small time step Δt, where this evolution depends on $\boldsymbol{\varepsilon}(0)$. Then, the state that results from this forward propagation, $|\psi(\Delta t)\rangle$, can be substituted into Eq. (14) to compute $\boldsymbol{\varepsilon}(\Delta t)$ associated with time $t = \Delta t$. This procedure is then repeated for all remaining time steps, where each forward step $k-1 \to k$ involves the following two computational steps *(i)* and *(ii)*:

(i) $|\psi(k\Delta t)\rangle = e^{-iH\left(\boldsymbol{\varepsilon}\left((k-1)\Delta t\right)\right)\Delta t}|\psi\left((k-1)\Delta t\right)\rangle$

(ii) $\boldsymbol{\varepsilon}(k\Delta t) = \mathbf{A}^{-1}\left(|\psi(k\Delta t)\rangle\right)\mathbf{b}\left(|\psi(k\Delta t)\rangle\right)$.

The computational details associated with steps *(i)* and *(ii)* are given in Sec. IV. As mentioned above, this procedure requires that $\mathbf{A}(t)$ is invertible at all times. A singularity is obtained when $\mathbf{A}(t)$ is not invertible, implying that $\det(\mathbf{A}(t)) = 0$. We proceed by investigating this case in more detail below.

From Eq. (12) it can be readily shown that the determinant of the matrix $\mathbf{A}$, suppressing the t-dependence, can

be written as

$$\det(\mathbf{A}) = (2\mu B)^3\Big(\big(\langle X^2\rangle + \langle Y^2\rangle\big)\big(\langle Y^2\rangle\langle X^2\rangle - \langle XY\rangle^2\big) + \big(\langle Y^2\rangle + \langle Z^2\rangle\big)\big(\langle Y^2\rangle\langle Z^2\rangle - \langle YZ\rangle^2\big) + \big(\langle Z^2\rangle + \langle X^2\rangle\big)\big(\langle X^2\rangle\langle Z^2\rangle - \langle XZ\rangle^2\big) + 2\big(\langle X^2\rangle\langle Y^2\rangle\langle Z^2\rangle - \langle XY\rangle\langle YZ\rangle\langle XZ\rangle\big)\Big) \geq 0 \tag{15}$$

The Cauchy-Schwarz inequalities between the state vectors $X|\psi(t)\rangle$, $Y|\psi(t)\rangle$, and $Z|\psi(t)\rangle$, which can be expressed in general as

$$\langle\varphi_1|\varphi_1\rangle\langle\varphi_2|\varphi_2\rangle \geq |\langle\varphi_1|\varphi_2\rangle|^2 \tag{16}$$

for any two state vectors $|\varphi_1\rangle$ and $|\varphi_2\rangle$, implies that Eq. (15) is positive semidefinite, as indicated. To see that this holds for the final line in Eq. (15), we begin with the following relations from Cauchy-Schwarz,

$$\begin{aligned}\langle X^2\rangle\langle Y^2\rangle &\geq \langle XY\rangle^2\\ \langle Y^2\rangle\langle Z^2\rangle &\geq \langle YZ\rangle^2\\ \langle Z^2\rangle\langle X^2\rangle &\geq \langle ZX\rangle^2\end{aligned} \tag{17}$$

which may be rearranged by taking products as,

$$\langle X^2\rangle^2\langle Y^2\rangle^2\langle Z^2\rangle^2 \geq \langle XY\rangle^2\langle YZ\rangle^2\langle ZX\rangle^2. \tag{18}$$

Taking the square root of both sides then yields the desired result that

$$\langle X^2\rangle\langle Y^2\rangle\langle Z^2\rangle \geq \langle XY\rangle\langle YZ\rangle\langle ZX\rangle. \tag{19}$$

The equality sign (i.e., a singularity) in Eq. (15) can arise if and only if $X|\psi(t)\rangle$, $Y|\psi(t)\rangle$, and $Z|\psi(t)\rangle$ are all linearly dependent. The QTC singularity issue will be addressed in Sec. IV below where we describe our computational methods for solving Eq. (14).

IV. COMPUTATIONAL METHODS

The numerical computation of the QTC fields according to Eq. (14) requires evaluations of the expectation values for the associated operators. Here, we study QTC of symmetric top molecules in the $|JKM\rangle$ eigenbasis of the drift Hamiltonian, which is given in Eq. (8) and can be rearranged as

$$H_0 = B\mathbf{J}^2 + (C-B)J_z^2 \tag{20}$$

leading to the eigenvalue equation

$$H_0\,|JKM\rangle = \big(BJ(J+1) + (C-B)K^2\big)|JKM\rangle \tag{21}$$

where $J = 0, 1, 2, \cdots$ is the total rotational angular momentum quantum number, $K = 0, \pm1, \pm2, \cdots, \pm J$ is the projection of the angular momentum onto the molecule-fixed z-axis, and $M = 0, \pm1, \pm2, \cdots, \pm J$ is the projection of the angular momentum onto the laboratory frame Z-axis. Eq. (21) can be obtained in a straightforward manner from Eq. (20) using the standard angular momentum matrix element relations $J_z|JKM\rangle = K|JKM\rangle$ and $\mathbf{J}^2|JKM\rangle = J(J+1)|JKM\rangle$. In this section, we obtain matrix element relations in this basis in order to carry out the two computational steps outlined in Sec. III that must be taken at each forward time step, i.e., *(i)* solving the time-dependent Schrödinger equation, Eq. (1) and *(ii)* solving the QTC equations, Eq. (14).

(i) Solving Eq. (1):

We begin by expanding the state of a symmetric top as

$$|\psi(t)\rangle = \sum_{JKM}\langle JKM|\psi(t)\rangle|JKM\rangle, \tag{22}$$

The expansion coefficients are governed by the equation

$$\begin{aligned} i\frac{d}{dt}&\langle JKM|\psi(t)\rangle\\ &= \sum_{J'K'M'}\langle JKM|H_0|J'K'M'\rangle\langle J'K'M'|\psi(t)\rangle\\ &- \sum_{J'K'M'}\mu\langle JKM|X|J'K'M'\rangle\langle J'K'M'|\psi(t)\rangle\varepsilon_X(t)\\ &- \sum_{J'K'M'}\mu\langle JKM|Y|J'K'M'\rangle\langle J'K'M'|\psi(t)\rangle\varepsilon_Y(t)\\ &- \sum_{J'K'M'}\mu\langle JKM|Z|J'K'M'\rangle\langle J'K'M'|\psi(t)\rangle\varepsilon_Z(t),\end{aligned} \tag{23}$$

where

$$\langle JKM|H_0|J'K'M'\rangle = BJ(J+1) + (C-B)K^2 \tag{24}$$

for $J' = J$, $K' = K$, and $M' = M$, and

$$\langle JKM|X|J'K'M'\rangle = -\frac{\mathcal{N}\sqrt{2}(-1)^{2+2J'+M'-K'+2M}}{2}\sum_{m=-1,1} m \begin{pmatrix} J & 1 & J' \\ M & m & -M' \end{pmatrix}\begin{pmatrix} J & 1 & J' \\ K & 0 & -K' \end{pmatrix},$$
$$\langle JKM|Y|J'K'M'\rangle = \frac{\mathcal{N}\sqrt{2}(-1)^{2+2J'+M'-K'+2M}}{2i}\sum_{m=-1,1} \begin{pmatrix} J & 1 & J' \\ M & m & -M' \end{pmatrix}\begin{pmatrix} J & 1 & J' \\ K & 0 & -K' \end{pmatrix}, \tag{25}$$

with $J' = J \pm 1$, $K' = K$, and $M' = M \pm 1$, and

$$\langle JKM|Z|J'K'M'\rangle = \mathcal{N}(-1)^{2+2J'+M'-K'+2M}\begin{pmatrix} J & 1 & J' \\ M & 0 & -M' \end{pmatrix}\begin{pmatrix} J & 1 & J' \\ K & 0 & -K' \end{pmatrix}, \tag{26}$$

with $J' = J \pm 1$, $K' = K$, and $M' = M$, in terms of $3j$ symbols, where $\mathcal{N} = \sqrt{(2J+1)(2J'+1)}$ [56–58]. The selection rules associated with Eqs. (25) and (26) can be used to accelerate the computation of the associated matrix elements. The selection rules also imply that fields coupling to the system via X, Y, Z can only be used to drive transitions in the quantum numbers J, M, while K is conserved.

(ii) Solving Eq. (14):

Eqs. (25) and (26) provide the matrix element relations needed for obtaining the elements of $\mathbf{A}(t)$ in the QTC Eq. (14) (i.e., see Eq. (12)) in the $|JKM\rangle$ eigenbasis. The computation of $\mathbf{b}(t)$ requires matrix element relations for the triple commutators of the form $[H_0, [H_0, \mathbf{R}]]$, i.e.,

$$\langle JKM|[H_0,[H_0,\mathbf{R}]]|J'K'M'\rangle = \Big(B\big(J(J+1) - J'(J'+1)\big)\Big)^2\langle JKM|\mathbf{R}|J'K'M'\rangle. \tag{27}$$

The issue of $\det(\mathbf{A}(t)) = 0$ in Eq. (15) can be clarified as follows [59]. We will show that the state vectors $X|\psi(t)\rangle$, $Y|\psi(t)\rangle$, and $Z|\psi(t)\rangle$ are linearly independent of each other. Specifically, $X|\psi(t)\rangle$, $Y|\psi(t)\rangle$, and $Z|\psi(t)\rangle$ can be, respectively, further written in terms of the basis $|JKM\rangle$, as

$$X|\psi(t)\rangle = \sum_{JKM}\Big[\sum_{J'K'M'}\langle JKM|X|J'K'M'\rangle\langle J'K'M'|\psi(t)\rangle\Big]|JKM\rangle,$$
$$Y|\psi(t)\rangle = \sum_{JKM}\Big[\sum_{J'K'M'}\langle JKM|Y|J'K'M'\rangle\langle J'K'M'|\psi(t)\rangle\Big]|JKM\rangle, \tag{28}$$

and

$$Z|\psi(t)\rangle = \sum_{JKM}\Big[\sum_{J'K'M'}\langle JKM|Z|J'K'M'\rangle\langle J'K'M'|\psi(t)\rangle\Big]|JKM\rangle, \tag{29}$$

which, from Eqs. (25) and (26), can be seen to be linearly independent, since the expansion coefficients for $X|\psi(t)\rangle$, $Y|\psi(t)\rangle$, and $Z|\psi(t)\rangle$ in the $|JKM\rangle$ basis are all distinct for bases truncated at some finite, albeit sufficiently large, value J_{max} (which is set to 30 in all of our calculations in Sec. VI). As a result, we conclude that $\det(\mathbf{A}(t)) > 0$ and that singularities will not appear when solving the QTC Eqs. (14).

V. REDUCTION TO THE CASE OF LINEAR MOLECULES

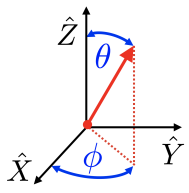

Figure 3. Diagram showing (θ, ϕ) relation between laboratory frame fixed $(\hat{X}, \hat{Y}, \hat{Z})$ coordinates (black) and molecular orientation vector (red)

Linear molecules possess only one axis of rotation and their Hamiltonian is given by,

$$H_0 = B\mathbf{L}^2 \tag{30}$$

where

$$\mathbf{L}^2 = -\left(\frac{1}{\sin\theta}\frac{\partial}{\partial\theta}\left(\sin\theta\frac{\partial}{\partial\theta}\right) + \frac{1}{\sin^2\theta}\frac{\partial^2}{\partial\phi^2}\right) \tag{31}$$

and has no explicit χ-dependence, as depicted in Fig. 3. This yields an expression for $\det(\mathbf{A})$ that is equal to Eq. (15). The matrix elements required to study QTC of linear molecules in their eigenbasis can be found using the matrix element relations obtained for symmetric tops and setting $K = 0$.

VI. NUMERICAL ILLUSTRATIONS

We have derived the QTC equations, Eq. (14), for controlling symmetric top orientation, and we now present numerical illustrations of this approach. For our illustrations, we consider the symmetric top molecule fluoromethane, with principal rotational constant $B = 5.182\,\text{cm}^{-1}$ and second rotational constant $C = 0.852\,\text{cm}^{-1}$ [60]. The magnitude of the dipole moment is given by $\mu = 1.847$ Debye [61]. The system is represented in the $|JKM\rangle$ basis, with basis elements $|000\rangle, \cdots, |30, \pm30, \pm30\rangle$. We consider designated tracks $\langle X\rangle_d(t)$, $\langle Y\rangle_d(t)$, and $\langle Z\rangle_d(t)$ given by

$$\begin{aligned}
\langle X\rangle_d(t) &\equiv 0.2e^{-\left(\frac{t-0.8T}{T/8}\right)^2}\sin(8Bt)\\
\langle Y\rangle_d(t) &\equiv 0.2e^{-\left(\frac{t-0.8T}{T/8}\right)^2}\cos(8Bt)\\
\langle Z\rangle_d(t) &\equiv 0.2e^{-\left(\frac{t-T}{T/8}\right)^2}\cos(8Bt)
\end{aligned} \tag{32}$$

where $T = 5/B$ is the terminal time and 30,000 time points are used for the calculations. Fig. 4 shows a 3D plot comparing these designated $\langle X\rangle_d(t)$, $\langle Y\rangle_d(t)$, and $\langle Z\rangle_d(t)$ trajectories with the actual tracks $\langle X\rangle(t)$, $\langle Y\rangle(t)$, and $\langle Z\rangle(t)$ that are followed when the molecule is initialized in $|\psi(0)\rangle = |000\rangle, |100\rangle, |110\rangle, |200\rangle$. We see that the curves in Fig. 4 are all superimposed, indicating that QTC is successful. Meanwhile, Fig. 5 shows the QTC fields determined via Eq. (14) that are found to drive $\langle X\rangle(t)$, $\langle Y\rangle(t)$, and $\langle Z\rangle(t)$ along these designated trajectories for the four initial conditions we consider, noting that the dominant frequency present ($\approx 9B$) is slightly higher than the dominant frequency in the associated tracks ($8B$). As per Sec. (V), the fields $\varepsilon_X(t)$, $\varepsilon_Y(t)$, and $\varepsilon_Z(t)$ and the tracks associated with $|\psi(0)\rangle =$

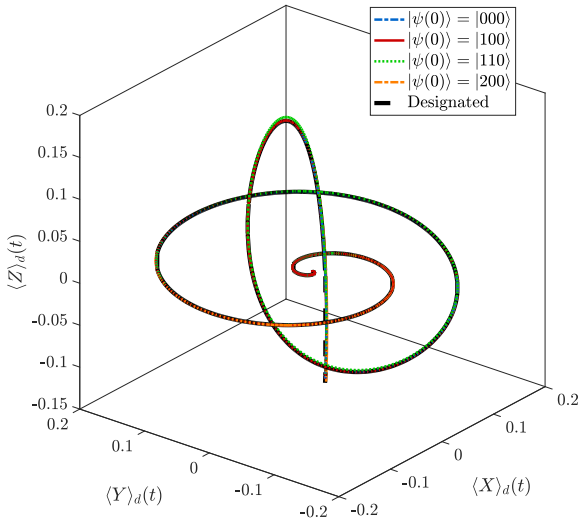

Figure 4. The designated tracks $\langle X\rangle_d(t)$, $\langle Y\rangle_d(t)$, and $\langle Z\rangle_d(t)$ given in Eq. (32) are plotted as a black curve inside of the $\langle X\rangle^2(t) + \langle Y\rangle^2(t) + \langle Z\rangle^2(t) = 1$ unit sphere. Then, the QTC tracks $\langle X\rangle(t)$, $\langle Y\rangle(t)$, and $\langle Z\rangle(t)$ followed by the system are plotted in color. The different colors correspond to different initial conditions $|\psi(0)\rangle = |000\rangle, |100\rangle, |110\rangle, |200\rangle$.

$|000\rangle, |100\rangle, |200\rangle$ are the same fields and tracks for a 3D linear rotor with rotational constant B, initialized as $|\psi(0)\rangle = |00\rangle, |10\rangle, |20\rangle$. We remark that in settings where it is desirable to obtain QTC fields that satisfy a zero-area constraint [62], the QTC fields for tracking an observable over some time interval $t \in [0, T]$ can be extended in time arbitrarily past $t = T$ to obtain a zero area pulse as desired (e.g., by mirroring the QTC field for time $t \in (T, 2T]$). However, when using such techniques, tracking control is only achieved over the original time interval $t \in [0, T]$.

VII. CONCLUSIONS

In this article, we have explored how QTC can be applied to design fields to orient symmetric top molecules, and have derived expressions for the QTC fields for driving the molecular orientation along time-dependent tracks. We also obtained matrix element relations to facilitate studying QTC of symmetric tops in the $|JKM\rangle$ symmetric top eigenbasis, and presented numerical illustrations of the QTC procedure for driving orientation dynamics in these systems. In order to realize associated experimental demonstrations, molecular rotors could be inves-

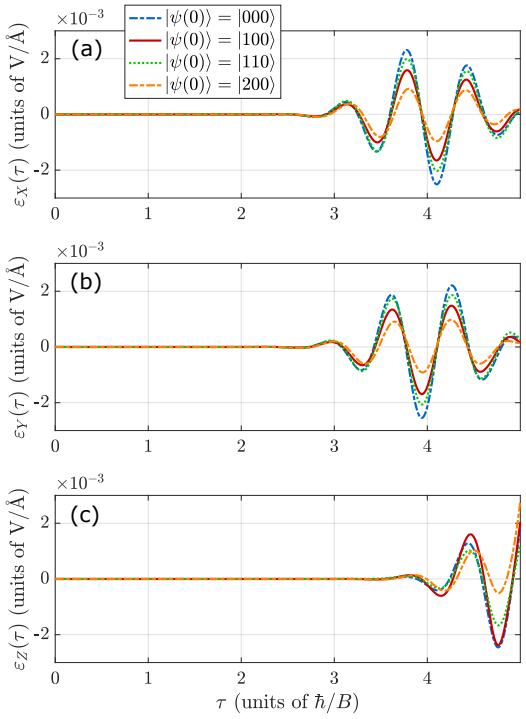

Figure 5. The QTC fields $\varepsilon_X(\tau)$, $\varepsilon_Y(\tau)$, and $\varepsilon_Z(\tau)$ are plotted as a function of the nondimensionalized time $\tau \equiv Bt$ in panels (a), (b), and (c), respectively. The different colors correspond to different initial conditions $|\psi(0)\rangle = |000\rangle, |100\rangle, |110\rangle, |200\rangle$.

tigated using, e.g., laser and evaporative cooling methods to create ultracold molecules, and then trapping them in an optical lattice [63]. Then, the creation of shaped microwave fields needed for QTC could be explored using arbitrary waveform generators [64, 65]. In these settings, noise in the fields that are generated will cause some deviation from the desired QTC field shapes. While previous work has found that QTC can be robust to control noise [27], carrying out careful analyses of the robustness of QTC fields for rotational control in the presence of realistic control noise would be a valuable direction of future research.

Looking ahead, this QTC formulation could be extended towards studying the control of so-called molecular superrotors [66], e.g. by selecting tracks to create very rapid rotational dynamics. Furthermore, the prospects of applying QTC towards the control of arrays of coupled molecular rotors, e.g. for applications in quantum information science [67–69], could be studied as well. For the latter, the study of coupled molecules will likely require high-dimensional modeling to represent the system dynamics, given that the model dimension scales exponentially in the number of degrees of freedom. As such, numerically exact simulations of coupled molecular rotors may not be computationally feasible. However, such challenges may be addressable through the use of suitable approximation frameworks for the quantum dynamics, e.g. [70–73].

ACKNOWLEDGMENTS

A.B.M. acknowledges support from the U.S. Department of Energy, Office of Science, Office of Advanced Scientific Computing Research, Department of Energy Computational Science Graduate Fellowship under Award No. DE-FG02-97ER25308, as well as support from Sandia National Laboratories' Laboratory Directed Research and Development Program under the Truman Fellowship. H.A.R. acknowledges support from DOE under Grant No. DE-FG02-02ER15344. T.S.H. acknowledges support from the Army Research Office W911NF-19-1-0382.

This article has been authored by an employee of National Technology & Engineering Solutions of Sandia, LLC under Contract No. DE-NA0003525 with the U.S. Department of Energy (DOE). The employee owns all right, title and interest in and to the article and is solely responsible for its contents. The United States Government retains and the publisher, by accepting the article for publication, acknowledges that the United States Government retains a non-exclusive, paid-up, irrevocable, world-wide license to publish or reproduce the published form of this article or allow others to do so, for United States Government purposes. The DOE will provide public access to these results of federally sponsored research in accordance with the DOE Public Access Plan https://www.energy.gov/downloads/doe-public-access-plan. Sandia National Laboratories is a multimission laboratory managed and operated by National Technology & Engineering Solutions of Sandia, LLC, a wholly owned subsidiary of Honeywell International Inc., for the U.S. Department of Energy's National Nuclear Security Administration under contract DE-NA0003525. This paper describes objective technical results and analysis. Any subjective views or opinions that might be expressed in the paper do not necessarily represent the views of the U.S. Department of Energy or the United States Government.

This report was prepared as an account of work sponsored by an agency of the United States Government. Neither the United States Government nor any agency thereof, nor any of their employees, makes any warranty, express or implied, or assumes any legal liability or re-

[1] C. Brif, R. Chakrabarti, and H. Rabitz, Control of quantum phenomena: past, present and future, New J. Phys. **12**, 075008 (2010).
[2] S. J. Glaser, U. Boscain, T. Calarco, C. P. Koch, W. Köckenberger, R. Kosloff, I. Kuprov, B. Luy, S. Schirmer, T. Schulte-Herbrüggen, D. Sugny, and F. K. Wilhelm, Training schrödinger's cat: quantum optimal control, Eur. Phys. J. D **69**, 279 (2015).
[3] C. P. Koch, Controlling open quantum systems: tools, achievements, and limitations, J. Phys. Condens. Matter **28**, 213001 (2016).
[4] A. P. Peirce, M. A. Dahleh, and H. Rabitz, Optimal control of quantum-mechanical systems: Existence, numerical approximation, and applications, Phys. Rev. A **37**, 4950 (1988).
[5] T. Caneva, T. Calarco, and S. Montangero, Chopped random-basis quantum optimization, Phys. Rev. A **84**, 022326 (2011).
[6] Y. Maday and G. Turinici, New formulations of monotonically convergent quantum control algorithms, J. Chem. Phys. **118**, 8191 (2003).
[7] W. Zhu and H. Rabitz, A rapid monotonically convergent iteration algorithm for quantum optimal control over the expectation value of a positive definite operator, J. Chem. Phys. **109**, 385 (1998).
[8] F. Dolde, V. Bergholm, Y. Wang, I. Jakobi, B. Naydenov, S. Pezzagna, J. Meijer, F. Jelezko, P. Neumann, T. Schulte-Herbrüggen, J. Biamonte, and J. Wrachtrup, High-fidelity spin entanglement using optimal control, Nat. Commun. **5**, 3371 (2014).
[9] G. Waldherr, Y. Wang, S. Zaiser, M. Jamali, T. Schulte-Herbrüggen, H. Abe, T. Ohshima, J. Isoya, J. F. Du, P. Neumann, and J. Wrachtrup, Quantum error correction in a solid-state hybrid spin register, Nature **506**, 204 (2014).
[10] E. S. Matekole, Y.-L. L. Fang, and M. Lin, Methods and results for quantum optimal pulse control on superconducting qubit systems, in *2022 IEEE International Parallel and Distributed Processing Symposium Workshops (IPDPSW)* (2022) pp. 600–606.
[11] M. Werninghaus, D. J. Egger, F. Roy, S. Machnes, F. K. Wilhelm, and S. Filipp, Leakage reduction in fast superconducting qubit gates via optimal control, npj Quantum Information **7**, 14 (2021).
[12] X. Wu, S. L. Tomarken, N. A. Petersson, L. A. Martinez, Y. J. Rosen, and J. L. DuBois, High-fidelity software-defined quantum logic on a superconducting qudit, Phys. Rev. Lett. **125**, 170502 (2020).
[13] P. Cerfontaine, T. Botzem, J. Ritzmann, S. S. Humpohl, A. Ludwig, D. Schuh, D. Bougeard, A. D. Wieck, and H. Bluhm, Closed-loop control of a gaas-based singlet-triplet spin qubit with 99.5% gate fidelity and low leakage, Nature communications **11**, 4144 (2020).
[14] C. Yang, K. Chan, R. Harper, W. Huang, T. Evans, J. Hwang, B. Hensen, A. Laucht, T. Tanttu, F. Hudson, *et al.*, Silicon qubit fidelities approaching incoherent noise limits via pulse engineering, Nature Electronics **2**, 151 (2019).
[15] A. Assion, T. Baumert, M. Bergt, T. Brixner, B. Kiefer, V. Seyfried, M. Strehle, and G. Gerber, Control of chemical reactions by feedback-optimized phase-shaped femtosecond laser pulses, Science **282**, 919 (1998).
[16] R. J. Levis, G. M. Menkir, and H. Rabitz, Selective bond dissociation and rearrangement with optimally tailored, strong-field laser pulses, Science **292**, 709 (2001).
[17] N. H. Damrauer, C. Dietl, G. Krampert, S. H. Lee, K. H. Jung, and G. Gerber, Control of bond-selective photochemistry in CH2BrCl using adaptive femtosecond pulse shaping, Eur. Phys. J. D **20**, 71 (2002).
[18] G. Vogt, G. Krampert, P. Niklaus, P. Nuernberger, and G. Gerber, Optimal control of photoisomerization, Phys. Rev. Lett. **94**, 068305 (2005).
[19] L. Levin, W. Skomorowski, L. Rybak, R. Kosloff, C. P. Koch, and Z. Amitay, Coherent control of bond making, Phys. Rev. Lett. **114**, 233003 (2015).
[20] P. Gross, H. Singh, H. Rabitz, K. Mease, and G. M. Huang, Inverse quantum-mechanical control: A means for design and a test of intuition, Phys. Rev. A **47**, 4593 (1993).
[21] Y. Chen, P. Gross, V. Ramakrishna, H. Rabitz, and K. Mease, Competitive tracking of molecular objectives described by quantum mechanics, J. Chem. Phys. **102** (1995).
[22] Y. Chen, P. Gross, V. Ramakrishna, H. Rabitz, K. Mease, and H. Singh, Control of Classical Regime Molecular Objectives -Applications of Tracking and Variations on the Theme*, Automatica **33**, 1617 (1997).
[23] R. Brockett and M. Mesarovic, The reproducibility of multivariable systems, J. Math. Anal. Appl. **11**, 548 (1965).
[24] R. M. Hirschorn, Invertibility of Nonlinear Control Systems, SIAM J. Control Optim. **17** (1979).
[25] C. K. Ong, G. M. Huang, T. J. Tarn, and J. W. Clark, Invertibility of quantum-mechanical control systems, Math. Systems Theory **17**, 335 (1984).
[26] D. A. Lidar and S. Schneider, Stabilizing qubit coherence

via tracking-control, Quantum Inf. Comput. **5** (2005).
[27] A. G. Campos, D. I. Bondar, R. Cabrera, and H. A. Rabitz, How to make distinct dynamical systems appear spectrally identical, Phys. Rev. Lett. **118**, 083201 (2017).
[28] A. Magann, T.-S. Ho, and H. Rabitz, Singularity-free quantum tracking control of molecular rotor orientation, Phys. Rev. A **98**, 043429 (2018).
[29] A. B. Magann, G. McCaul, H. A. Rabitz, and D. I. Bondar, Sequential optical response suppression for chemical mixture characterization, Quantum **6**, 626 (2022).
[30] G. McCaul, C. Orthodoxou, K. Jacobs, G. H. Booth, and D. I. Bondar, Controlling arbitrary observables in correlated many-body systems, Phys. Rev. A **101**, 053408 (2020).
[31] G. McCaul, C. Orthodoxou, K. Jacobs, G. H. Booth, and D. I. Bondar, Driven imposters: Controlling expectations in many-body systems, Phys. Rev. Lett. **124**, 183201 (2020).
[32] G. McCaul, A. F. King, and D. I. Bondar, Optical indistinguishability via twinning fields, Phys. Rev. Lett. **127**, 113201 (2021).
[33] S. Zou, Q. Ren, G. G. Balint-Kurti, and F. R. Manby, Analytical control of molecular excitations including strong field polarization effects, Phys. Rev. Lett. **96**, 243003 (2006).
[34] S. Zou, C. Sanz, and G. G. Balint-Kurti, Coherent control of molecular alignment of homonuclear diatomic molecules by analytically designed laser pulses, J. Chem. Phys. **129** (2008).
[35] A. Tóth and A. Csehi, Strong-field control by reverse engineering, Phys. Rev. A **104**, 063102 (2021).
[36] W. Zhu, M. Smit, and H. Rabitz, Managing singular behavior in the tracking control of quantum dynamical observables, J. Chem. Phys. **110** (1999).
[37] R. Hirschornf and J. Davis, Output Tracking for Nonlinear Systems with Singular Points, SIAM J. Control Optim. **25** (1987).
[38] C. P. Koch, M. Lemeshko, and D. Sugny, Quantum control of molecular rotation, Rev. Mod. Phys. **91**, 035005 (2019).
[39] P. M. Kraus, A. Rupenyan, and H. J. Wörner, Phys. Rev. Lett. **109**, 233903 (2012).
[40] P. R. Brooks, Science **193**, 11 (1976).
[41] R. N. Zare, Science **279**, 1875 (1998).
[42] T. P. Rakitzis, A. J. van den Brom, and M. H. M. Janssen, Science **303**, 1852 (2004).
[43] S. De, I. Znakovskaya, D. Ray, F. Anis, N. G. Johnson, I. A. Bocharova, M. Magrakvelidze, B. D. Esry, C. L. Cocke, I. V. Litvinyuk, and M. F. Kling, Field-free orientation of co molecules by femtosecond two-color laser fields, Phys. Rev. Lett. **103**, 153002 (2009).
[44] K. Oda, M. Hita, S. Minemoto, and H. Sakai, All-optical molecular orientation, Phys. Rev. Lett. **104**, 213901 (2010).
[45] S. Fleischer, Y. Zhou, R. W. Field, and K. A. Nelson, Molecular orientation and alignment by intense single-cycle thz pulses, Phys. Rev. Lett. **107**, 163603 (2011).
[46] K. Hoki and Y. Fujimura, Chem. Phys. **267**, 187 (2001).
[47] J. Salomon, C. M. Dion, and G. Turinici, J. Chem. Phys. **123**, 144310 (2005).
[48] G. Turinici and H. Rabitz, J. Phys. A **43**, 105303 (2010).
[49] M. Yoshida and Y. Ohtsuki, Chem. Phys. Lett. **633**, 169 (2015).
[50] H. Yu, T.-S. Ho, and H. Rabitz, Phys. Chem. Chem. Phys. **20**, 13008 (2018).
[51] T. Szidarovszky, M. Jono, and K. Yamanouchi, Limao: Cross-platform software for simulating laser-induced alignment and orientation dynamics of linear-, symmetric-and asymmetric tops, Comput. Phys. Commun. **228**, 219 (2018).
[52] A. Ma, A. B. Magann, T.-S. Ho, and H. Rabitz, Optimal control of coupled quantum systems based on the first-order magnus expansion: Application to multiple dipole-dipole-coupled molecular rotors, Phys. Rev. A **102**, 013115 (2020).
[53] U. Boscain, M. Caponigro, and M. Sigalotti, Multi-input schrödinger equation: controllability, tracking, and application to the quantum angular momentum, J. Differ. Equ. **256**, 3524 (2014).
[54] U. Boscain, E. Pozzoli, and M. Sigalotti, Classical and quantum controllability of a rotating symmetric molecule, SIAM J Control Optim. **59**, 156 (2021).
[55] R. N. Zare, *Angular momentum : understanding spatial aspects in chemistry and physics* (Wiley, New York ; Toronto, 1988).
[56] P. C. Cross, R. M. Hainer, and G. W. King, The asymmetric rotor ii. calculation of dipole intensities and line classification, J. Chem. Phys. **12**, 210 (1944).
[57] R. N. Zare, Molecular level-crossing spectroscopy, J. Chem. Phys. **45**, 4510 (1966).
[58] H. W. Kroto, *Molecular Rotation Spectra* (Dover Publications, Inc, New York, 1992).
[59] The following analysis is missing in our preceding article [28], but analogous arguments hold. We also note that the coefficient prefactor in Eq. (12) of [28] should read $\frac{1}{D(\varphi,t)}\frac{\hbar^2}{2\mu B}$.
[60] D. Papousek, Y. Hsu, H. Chen, P. Pracna, S. Klee, and M. Winnewisser, Far infrared spectrum and ground state parameters of 12ch3f, Journal of Molecular Spectroscopy **159**, 33 (1993).
[61] B. Starck, R. Tischer, and M. Winnewisser, Molecular constants from microwave, molecular beam, and electron spin resonance spectroscopy · 1 introduction: Datasheet from landolt-börnstein - group ii molecules and radicals · volume 6: "molecular constants from microwave, molecular beam, and electron spin resonance spectroscopy" in springermaterials (https://doi.org/10.1007/10201226_1), copyright 1974 Springer-Verlag Berlin Heidelberg.
[62] C.-C. Shu, T.-S. Ho, and H. Rabitz, Monotonic convergent quantum optimal control method with exact equality constraints on the optimized control fields, Phys. Rev. A **93**, 053418 (2016).
[63] M. A. Baranov, M. Dalmonte, G. Pupillo, and P. Zoller, Condensed Matter Theory of Dipolar Quantum Gases, Chem. Rev. **112**, 5012 (2012).
[64] J. Yao, Photonic generation of microwave arbitrary waveforms, Opt. Commun. **284**, 3723 (2011).
[65] I. Lin, J. McKinney, and A. Weiner, Photonic synthesis

of broadband microwave arbitrary waveforms applicable to ultra-wideband communication, IEEE Microw. Wirel. Compon. Lett **15**, 226 (2005).
[66] A. Korobenko, A. A. Milner, and V. Milner, Direct observation, study, and control of molecular superrotors, Phys. Rev. Lett. **112**, 113004 (2014).
[67] D. DeMille, Phys. Rev. Lett. **88**, 067901 (2002).
[68] L. Bomble, P. Pellegrini, P. Ghesquière, and M. Desouter-Lecomte, Phys. Rev. A **82**, 062323 (2010).
[69] Q. Wei, Y. Cao, S. Kais, B. Friedrich, and D. Herschbach, ChemPhysChem **17**, 3714 (2016).
[70] M. Messina, K. R. Wilson, and J. L. Krause, Quantum control of multidimensional systems: Implementation within the time?dependent hartree approximation, J. Chem. Phys. **104**, 173 (1996).
[71] M. Schröder, J.-L. Carreón-Macedo, and A. Brown, Implementation of an iterative algorithm for optimal control of molecular dynamics into mctdh, Phys. Chem. Chem. Phys. **10**, 850 (2008).
[72] A. Magann, L. Chen, T.-S. Ho, and H. Rabitz, Quantum optimal control of multiple weakly interacting molecular rotors in the time-dependent hartree approximation, J. Chem. Phys. **150**, 164303 (2019).
[73] P. Doria, T. Calarco, and S. Montangero, Optimal control technique for many-body quantum dynamics, Phys. Rev. Lett. **106**, 190501 (2011).